



# Liquefaction potential for the Kathmandu Valley, Nepal: a sensitivity study

Rama M. Pokhrel<sup>1</sup> · Charlotte E. L. Gilder<sup>1</sup> · Paul J. Vardanega<sup>1</sup> ·  
Flavia De Luca<sup>1</sup> · Raffaele De Risi<sup>1</sup> · Maximilian J. Werner<sup>2</sup> ·  
Anastasios Sextos<sup>1</sup>

Received: 2 December 2020 / Accepted: 9 August 2021 / Published online: 23 September 2021  
© The Author(s) 2021

## Abstract

An assessment of liquefaction potential for the Kathmandu Valley considering seasonal variability of the groundwater table has been conducted. To gain deeper understanding seven historical liquefaction records located adjacent to borehole datapoints (published in SAFER/GEO-591) were used to compare two methods for the estimation of liquefaction potential. Standard Penetration Test (SPT) blowcount data from 75 boreholes inform the new liquefaction potential maps. Various scenarios were modelled, i.e., seasonal variation of the groundwater table and peak ground acceleration. Ordinary kriging, implemented in ArcGIS, was used to prepare maps at urban scale. Liquefaction potential calculations using the methodology from (Sonmez, Environ Geol 44:862–871, 2003) provided a good match to the historical liquefaction records in the region. Seasonal variation of the groundwater table is shown to have a significant effect on the spatial distribution of calculated liquefaction potential across the valley. The less than anticipated liquefaction manifestations due to the Gorkha earthquake are possibly due to the seasonal water table level.

**Keywords** Kathmandu Valley · Seismic hazard · Liquefaction potential · Groundwater table · Kriging

## 1 Introduction

The Kathmandu Valley is located approximately 10 km from the Main Himalayan Thrust (MHT) (Elliott et al. 2016). This geographical area experienced several destructive earthquakes in the past: the latest significant event occurred in 2015, the  $M_w$  7.8 Gorkha earthquake (Grandin et al. 2015). The Gorkha earthquake caused structural damage and geotechnical failures, including landslides and liquefaction (e.g., Goda et al. 2015; Chiaro et al. 2015; Hashash et al. 2015; Moss et al. 2015; Sharma and Deng 2019). The thick, sediments underlying the Kathmandu Valley have highly variable geotechnical properties (e.g., Sakai et al. 2008; Gilder et al. 2020) and are prone to liquefy (e.g., Rajendran et al.

---

✉ Paul J. Vardanega  
p.j.vardanega@bristol.ac.uk

Extended author information available on the last page of the article

2016). However, the study of Moss et al. (2017) demonstrated that evidence of liquefaction in the aftermath of the 2015 Gorkha earthquake was less significant than expected. Possible reasons for this may include: changes in the groundwater table due to extraction (e.g., Pandey et al. 2012); seasonal variation of groundwater table level (Shrestha and Tamrakar 2018) and/or underestimation of soil stiffness (e.g.,  $V_{S30}$ ) (cf. Wald and Allen 2007). Jha et al. (2020) compared probabilistic and deterministic approaches for liquefaction potential evaluation in the Kathmandu Valley using two boreholes. In this paper, two deterministic approaches (Iwasaki et al. 1978, 1982, 1984 and Sonmez 2003) are compared using a database of field observations. The observations of Moss et al. (2017) are also tested in this paper.

For the Kathmandu Valley, geotechnical testing (Gilder et al. 2019a; Pokhrel et al. 2019a) and the collection of historical geotechnical investigations (Gilder et al. 2020) have shown that the slope-based prediction of shear wave velocity represents an overestimation for many areas of the valley (Gilder et al. 2018; De Risi et al. 2021). In data-scarce regions, such as the Kathmandu Valley, geostatistical tools may be used to extrapolate results from point locations to a geographical area (e.g., De Risi et al. 2021). Kriging interpolation is often used to determine values for liquefaction potential measures at locations without sufficient geotechnical data (e.g., Baise and Lenz 2006; Maruyama et al. 2010; Pokhrel et al. 2010, 2013, 2012; Thompson et al. 2010; Chung and Rogers 2011; Baker and Faber 2008; Liu and Chen 2006, 2010; Habibullah et al. 2012).

Three new records of liquefaction and four previously documented records of liquefaction within the Kathmandu Valley are examined in this paper. These records are all located in the vicinity of borehole locations collected in the geo-database SAFER/GEO-591 (Gilder et al. 2019b, 2020). In this paper, the two reviewed approaches for liquefaction potential determination use the triggering model from Seed and Idriss (1971) and the manifestation models by Iwasaki et al. (1978, 1982, 1984) and Sonmez (2003) respectively. These approaches are compared against the liquefaction records examined in this study to enable comment on which is the most applicable ‘simplified’ method for the valley. The approaches are implemented using data from 75 borehole locations (see Table 1) along with the kriging algorithm from ArcGIS to prepare liquefaction maps for variable PGA values and groundwater table levels. Another possible use of SAFER/GEO-591 is to use the data to estimate building settlements (based on SPT  $N_{60}$ ) using methodologies such as that described in Valverde-Palacios et al. (2014).

## 2 The Kathmandu Valley

### 2.1 Geology

The Kathmandu Valley is an intermontane basin in the Lesser Himalayas in central Nepal, south of the Great Himalayan Range (e.g., Sakai et al. 2008). The valley is made up of: (a) a basement, metamorphic rock underlying the valley at depth, and (b) younger valley sediments which overly the metamorphic rock formations. Figure 1 shows the liquefaction map of the UNDP/UNCHS (HABITAT) (1993) Subproject “Seismic hazard mapping and risk assessment for Nepal”. This project was important as new surficial geological maps were developed based on the details of well data sources originating from the early work done in the Valley. Similarly, the geomorphological map of Yoshida and Igarashi (1984) (Fig. 1b) described a number of sediments resulting from both the Quaternary deposition (recent

**Table 1** Boreholes SAFER/  
GEO-591 (Gilder et al. 2019b)  
used in this study

No	BH_ID
1	R_JICA_2002_BH1
2	R_JICA_2002_BH2
3	R_JICA_2002_BH3
4	R_JICA_2002_BH4
5	R_JICA_2002_BH5
6	RES_Pokh_2006_BH6
7	RES_Pokh_2006_BH7
8	RES_Safe_2018_BH1
9	RES_Safe_2018_BH2
10	IND_Bans_2007_BH1
11	IND_Bakh_2006_BH3
12	R_JRAP_2016_BH4
13	R_JRAP_2016_BH2
14	R_JRAP_2016_BH5
15	R_JRAP_2016_BH3
16	R_JRAP_2016_BH1
17	IND_Sina_2006_BH1
18	IND_Chan_2007_BH4
19	IND_Biju_1000_BH1
20	IND_Dhob_1000_BH2
21	IND_Bhat_2008_BH2
22	IND_Sane_2007_BH1
23	IND_Taha_2007_BH11
24	IND_Ravi_2008_BH1
25	IND_Solt_2007_BH1
26	IND_Dhum_2007_BH2
27	IND_Pani_2008_BH1
28	IND_Lazi_2008_BH3
29	IND_Kule_2007_BH1
30	IND_Sane_1000_BH3
31	IND_Kupo_1000_BH1
32	IND_Sank_2008_BH1
33	IND_Kama_2008_BH1
34	IND_Pulc_2008_BH1
35	IND_Solt_2008a_BH1
36	IND_Dill_2008_BH2
37	IND_Gyan_2008_BH2
38	IND_Sane_2009_BH5
39	IND_Bish_2007_BH5
40	IND_Sano_2008_BH2
41	IND_Sane_1001_BH1
42	IND_Hatt_1000_BH6
43	IND_Balk_2009_BH2
44	IND_Sane_1002_BH1
45	IND_Dhap_2009_BH1
46	IND_Ghat_2009_BH4
47	IND_Kada_1000_BH10
48	IND_Sane_2009a_BH3
49	IND_Thad_2009_BH1

**Table 1** (continued)

No	BH_ID
50	IND_Baba_2008_BH2
51	IND_Balk_2009a_BH2
52	IND_Batt_2005_BH3
53	IND_Solt_2008_BH1
54	IND_Naxa_1000_BH1
55	IND_Naxa_1000_BH2
56	IND_Naxa_1000_BH3
57	IND_Hanu_1002_BH1
58	IND_Hanu_1002_BH2
59	IND_Balk_2009b_F2
60	IND_Dhap_2008_BH9
61	IND_Bakh_2006_BH1
62	IND_Jaga_2010_BH1
63	IND_Kote_2008_BH1
64	IND_Kaus_2017_BH1
65	IND_Kaus_2017_BH2
66	IND_Kaus_2017_BH3
67	IND_Goda_2018_BH1
68	IND_Bala_2018_BH1
69	IND_Chys_2015_BH1
70	RES_Daha_2002_BH4
71	RES_Pagl_2018_BH1
72	RES_Kate_1996_T2
73	RES_Kate_1996_R1
74	Bungmati-1 (Jha et al. 2020)
75	Bungmati-2 (Jha et al. 2020)

sediment deposits near rivers) and earlier Pliocene to Pleistocene deposits from a variety of depositional environments including fluvio-deltaic, lacustrine and deltaic (Sakai et al. 2008).

The geological map in Fig. 2 indicates the newer geological designations from Shrestha et al. (1998). The Kalimati Formation beneath any recent deposits in the central Valley (Fig. 1c) (Paudel and Sakai 2009) often consists of a laminated black clayey, silt inter-laminated with silt, clay and with very fine, silty, sand layers. The Sunakothi Formation, present in much of the southern part of the Valley, contains both clayey sequences and laminated silts and sands. The Terrace deposits contain coarser materials, skirting the bed-rock geology of the southern central and western margins. When examining Fig. 1b, it can be seen how the original liquefaction map (Fig. 1a) was defined. Where rivers are present (with presumably saturated soils) these areas represent the position of highest liquefaction potential. This potential reduces towards the valley edge. More recent assessments have indicated that the highest potential is at locations near the rivers and in the central valley (Gautam et al. 2017), and probabilistic assessments have reported similar findings (Sajan et al. 2020; Khatakho et al. 2021). However, this has been attributed to the older sequences and as the Valley contains a complex mix of laminated sequences it remains a challenge to evaluate the liquefaction potential in the valley. It is likely much of the valley mapping is affected by recent superficial deposits (which are not currently shown on maps) due to

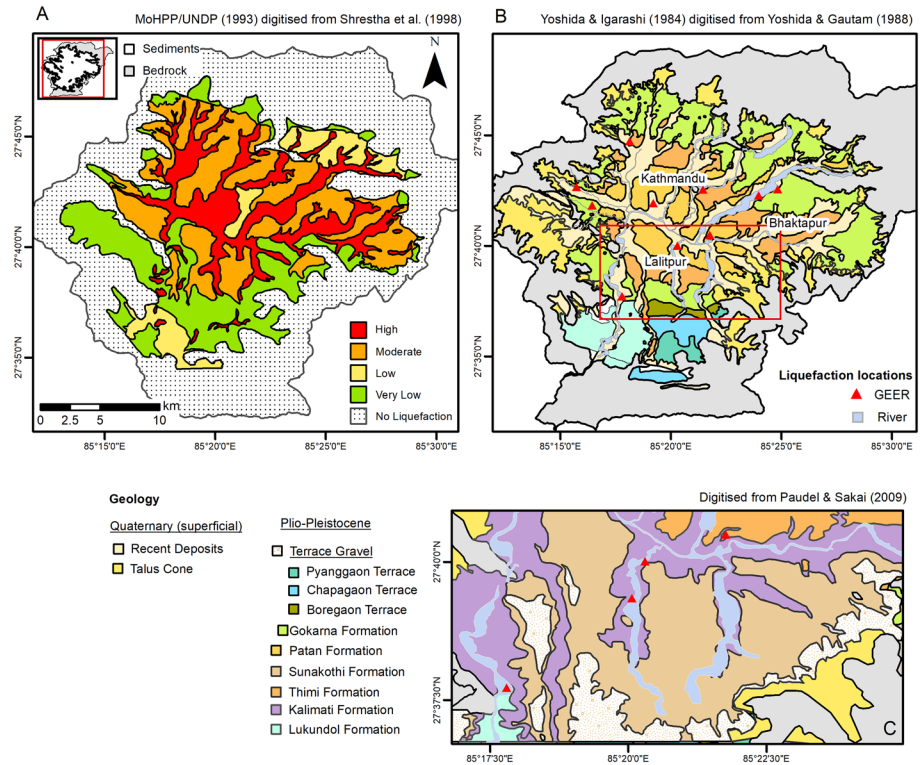


**Fig. 1** a Liquefaction map, UNDP/UNCHS (HABITAT) (1993), digitised map data from Shrestha et al. (1998) b Kathmandu Valley sediments based on geomorphological distribution from Yoshida and Igarashi (1984), digitised map data from Yoshida and Gautam (1988) c map of Plio-Pleistocene sediments, digitised map data from Paudel and Sakai (2009)

the likely occurrence of channel movement and geomorphic development of the river basin (Shrestha and Tamrakar 2013). Age relationships of the soils shown in Fig. 1 are inexact due to the combination of map sources. For instance, more recent Cone Penetration Testing (CPT) work has suggested that some locations near rivers are unlikely to liquefy (Gilder et al. 2021) but also the position of the Araniko Highway movement is upon a relict river channel. These conclusions (Gilder et al. 2021) are also currently affected by the ability to assess the silts of this region for liquefaction potential due to the limited amount of geotechnical field and laboratory testing. Herein, the aim is to improve understanding of potential seasonal variation of liquefaction potential and to compare the modelled results to observations taken following the 2015 Gorkha earthquake.

## 2.2 Historical earthquakes and faults

Table 2 lists the significant historical earthquakes recorded in the Kathmandu Valley. The most devastating earthquakes occurred in 1833, 1866, 1934, 1988, and 2015 (Rana 1935; Bilham 1995, 2019; Pandey et al. 2002; Pandey and Molnar 1988; Goda et al. 2015). Prior studies considered a fault system containing three main faults, namely the main central thrust (MCT), main boundary thrust (MBT) and himalayan frontal thrust (HFT) (e.g.,

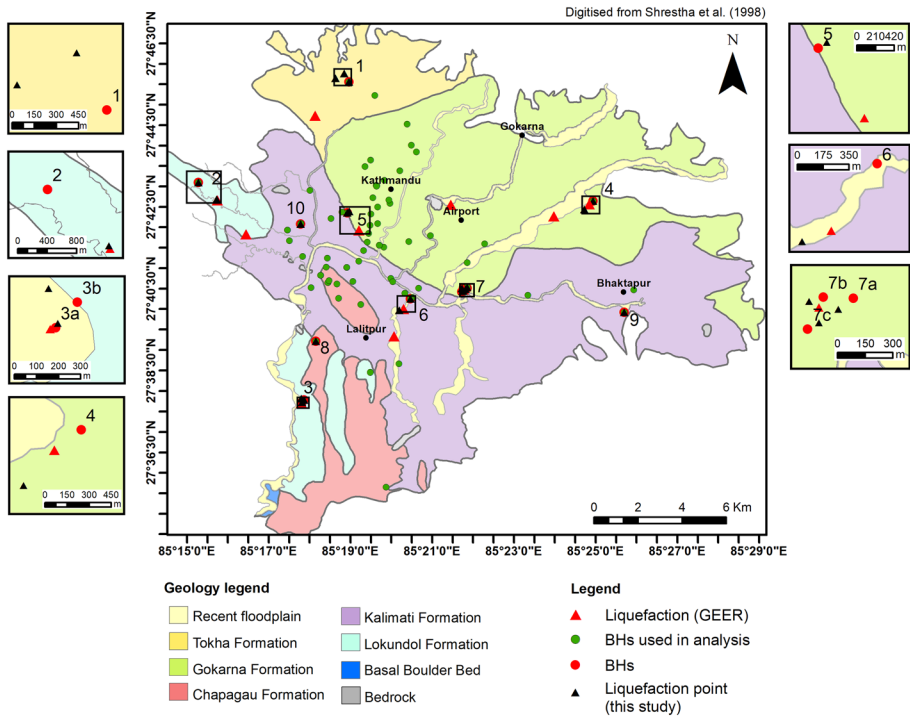


**Fig. 2** Engineering geological map with liquefaction validations points indicated with the IDs provided in Table 6 and zoomed areas to indicate distance between the liquefaction point identified in this study (black triangle) and validation borehole (red circle). The historical liquefaction points evidenced by the field study Geotechnical Extreme Event Reconnaissance (GEER) (locations given in Hashash et al. 2015) are also shown (red triangles). Recent deposits have been added to map data digitised from Shrestha et al. (1998) map to reflect true extent of rivers

**Table 2** Historical earthquakes that caused severe damage in the Kathmandu Valley

Date	Moment magnitude ( $M_w$ )	Location	References
August 26, 1833	7.8	North of Kathmandu Valley	Pandey and Molnar (1988); Bilham (1995)
May 23, 1866	7.0	North of Kathmandu	Szeliga et al. (2010)
Jan 15, 1934	8.4	Udayapur, Nepal	Rana (1935); Chen and Molnar (1977)
August 21, 1988	6.5	Udayapur, Nepal	Bilham (2019)
April 25, 2015	7.8	Gorkha, Nepal	Goda et al. (2015)
May 13, 2015	7.3	Kodari, Nepal	Goda et al. (2015)

Chaulagain et al. 2015). The maximum PGA generated for the Kathmandu Valley by the earthquakes from these thrusts is around 0.35 g; consistent with the old building code of Nepal (1994) (NBC 1994). Publications after the 2015 Gorkha earthquake have better described the geometry of the main himalayan thrust (MHT) beneath the Kathmandu

Valley (Elliott et al. 2016) and highlighted that the MHT could generate an earthquake as great as magnitude  $M_w$  9.0 (Stevens et al. 2018; Pokhrel et al. 2019b). The new building code for Nepal (NBC 2020), specifies a maximum PGA value for the Kathmandu valley of 0.35 g for a 475-year return period. PSHA results are significantly affected by the specific choice of GMPEs assumed (Stevens et al. 2018; De Risi et al. 2020). Taking the MHT as a single seismogenic source, the PGA can vary significantly depending on the GMPE used.

### 2.3 Groundwater level and water table

Nepal lies in a humid-subtropical climatic region with dry-winters (Kottek et al. 2006) and heavy rain-summers. During the rainy seasons, monsoons last from mid-June to mid-September (approximately 90 days) during which time the average rainfall is more than 1000 mm (Pokharel and Hallett 2015). The large population of 2.5 million (CBS 2012) living in the Kathmandu Valley use groundwater for domestic and commercial purposes. If consumption exceeds the recharge of the groundwater in the dry season, the change in height of the groundwater table at the end of this season can be as much as 5 m (e.g., Shrestha and Tamrakar 2018). According to Moss et al. (2017), groundwater withdrawal in the Kathmandu Valley over the last decades resulted in a drop of the average water table in the valley. This is also supported by Pandey et al. (2012), who reported that 60–70% of the water supply during the dry season comes from groundwater with a consequent drawdown up to 7.5 m from 2000 to 2008. Moss et al. (2017) estimated an average annual groundwater drawdown of roughly 1 m per year and assumed a variable water table depth derived from the global water table database by Fan et al. (2013). For the purposes of liquefaction assessment the Moss et al. (2017) groundwater model ranged between 0 and 40 m within the sediment deposits in the central Valley. However, the seasonal variation of the groundwater table for particular deposits was not explicitly considered.

Shrestha and Tamrakar (2018) mapped the shallow groundwater level for dry (pre-monsoon) and wet (monsoon) season in the northern part of the Kathmandu Valley. In particular, data from 239 wells were collected during wet and dry season, allowing an average estimation of seasonal variation of the groundwater level. In this study, using the observations of Shrestha and Tamrakar (2018):

- 1.6 m is taken as the approximate value for the water table in the wet season, estimating it as the average depth minus one half of the standard deviation from the data reported in Shrestha and Tamrakar (2018).
- 5.1 m is taken as the approximate value for the water table in the dry season, estimating it as the average depth plus one half of the standard deviation from the data reported in Shrestha and Tamrakar (2018).

These assumptions do not allow for the spatial variation of the groundwater table (cf. Fan et al. 2013). However, the aim herein is to study seasonal variation of the groundwater table in conjunction with variability of the PGA as obtained from recent probabilistic hazard assessment studies.

### 3 Methodology

#### 3.1 Liquefaction potential calculation

Seed and Idriss (1971) proposed a method to assess liquefaction resistance of soils. In this approach, the factor of safety against liquefaction ( $F_L$ ) is determined by the ratio between the cyclic resistance ratio (CRR) and the earthquake-induced cyclic stress ratio (CSR) (see Sonmez (2003) for further commentary on the historical development of this approach). This method is widely used as a triggering model to evaluate the factor of safety against liquefaction  $F_L$  (e.g., Geyin et al. 2020).  $F_L$  is used to evaluate if a soil layer is susceptible or non-susceptible to liquefaction during an earthquake.

Iwasaki et al. (1984) proposed a liquefaction potential index ( $I_L$ ) to evaluate the liquefaction potential in multiple layers of soil. The liquefaction potential index ( $I_L$ ) in Iwasaki et al. (1984) is referred to in this paper as the liquefaction potential ( $P_L$ ); this parameter assumes that surface manifestation depends on the thicknesses of all strata that can liquefy in the uppermost 20 m of a soil column, their proximity to the ground surface, and the amount by which the factor of safety against liquefaction in each stratum ( $F_L$ ) is less than 1.0 (Geyin et al. 2020). The methodology of Iwasaki et al. (1984) was also used in the work of Piya et al. (2004) who presented both qualitative and quantitative liquefaction potential assessments for the Kathmandu valley using the available SPT data at that time.

Equation 1 gives the function of the liquefaction resistance factor,  $F(z)$ , is expressed through Eq. 2 and the depth weighting factor,  $W(z)$ , is expressed through Eq. 3 in which  $z$  represents the depth of the midpoint of the soil layer from the surface.

$$P_L = \int_0^{20} F(z) \cdot W(z) dz \quad (1)$$

$$F(z) = \begin{cases} 1 - F_L & \text{for } F_L \leq 1 \\ 0 & \text{for } F_L > 1 \end{cases} \quad (2)$$

$$W(z) = \begin{cases} 10 - 0.5 \cdot z & \text{for } z \leq 20m \\ 0 & \text{for } z > 20m \end{cases} \quad (3)$$

Sonmez (2003) modified  $P_L$  based on data from Inegol (Turkey) and Sonmez and Gokceoglu (2005) modified  $P_L$  based on data from Yuanlin (Taiwan). The assumption for  $F(z)$  to be used in Eq. 1 was modified according to Eq. 4 to incorporate marginally liquefiable strata ('moderate') (characterised by  $F_L$  in the range [0.95–1.2], Sonmez (2003)).

$$F(z) = \begin{cases} 1 - F_L & \text{for } F_L \leq 0.95 \\ 2 \cdot 10^6 \cdot e^{-18.427F_L} & \text{for } 0.95 < F_L < 1.2 \\ 0 & \text{for } F_L \geq 1.2 \end{cases} \quad (4)$$

Comparison of the approaches of Iwasaki et al. (1984) and Sonmez (2003) was also presented in Liu (2008). In the present study, the methodologies by Iwasaki et al. (1984) and Sonmez (2003) were used to evaluate the liquefaction potential in the Kathmandu valley using new case evidence from the Gorkha earthquake and geotechnical investigations from



**Table 3** Summary of the mean  $D_{50}$  and  $\rho_{soil}$  values for Kathmandu Valley from SAFER/GEO-591 (Gilder et al. 2019b);  $n$  = number of data points used to compute the stated averages

Soil Type	SAFER/GEO-591					
	$D_{50}$ (mm)			$\rho_{soil}$ (g/cm <sup>3</sup> )		
	mean	n	min	mean	max	n
Surface soil	–	–	–	–	–	–
Clay	–	–	1.49	1.75	1.99	22
Silt	0.011	11	1.54	1.82	2.19	17
Sandy silt	0.041	6				
Silty sand	–	–	1.65	1.88	2.28	122
Fine sand	0.380	27				
Medium sand						
Coarse sand						
Gravelly sand	0.710	5	–	–	–	–

the SAFER/GEO-591 geo-database (Gilder et al. 2019b). Table 3 shows the  $D_{50}$  and  $\rho_{soil}$  values used for the liquefaction potential analysis. Figure 3 shows the grain-size distribution curves from the SAFER/GEO-591 geo-database against the “liquefiable” and “potentially liquefiable” bounds from Tsuchida (1970) and Koester and Tsuchida (1988). These distribution curves are mainly concentrated in the liquefiable boundary emphasising a potential for high susceptibility.

### 3.2 Historical records of liquefaction in the Kathmandu Valley

Photographs taken immediately after the Nepal-Bihar earthquake show fractures developed in the field associated with sand boiling (Rana 1935). After the Nepal-Bihar earthquake, eyewitness accounts describe liquefaction evidenced by observations of sand boiling and soil fissuring. Photographic reports from Rana (1935) show “ground fissures after sand boiling” in the central part of Kathmandu city (location 5 in Fig. 2), in Tundikhel (Rana 1935). Similarly, during the 2015 Gorkha earthquake further evidence was observed. Table 4 details seven documented liquefaction records in the Kathmandu Valley which are

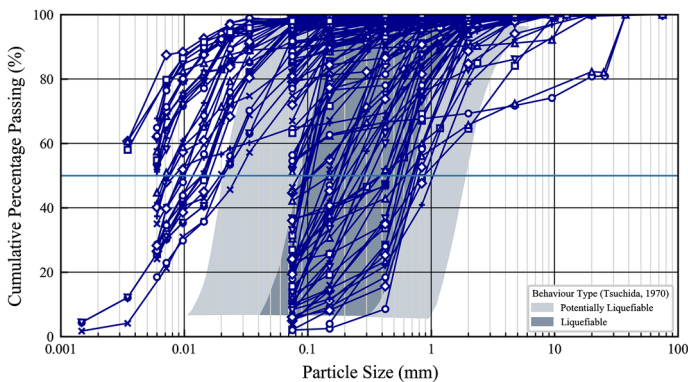


**Fig. 3** Grain-size distribution curves from SAFER/GEO-591, liquefaction bounds attributed to Tsuchida (1970) digitized from Koester and Tsuchida (1988)

**Table 4** Approximate liquefaction evidence point co-ordinates and evidence details extracted from GEER report (Hashash et al. 2015)

Location	Latitude °N	Longitude °E	Evidence (page(s) reference from Hashash et al. 2015)
Ramkot	27.711025	85.26229	106–108
Singa Durbar Bridge	27.698793	85.32006	108–109
Manamajju	27.745523	85.302223	109–110
Guheshwor	27.709253	85.357553	110–111
Lokanthali	27.674816	85.362646	111–118
Syuchatar	27.697230	85.274080	118–119
Bungamati	27.628630	85.296650	119
Changu Narayan	27.709430	85.413970	120
Mulpani	27.704575	85.399617	121
Gwarko/Imadol	27.666782	85.338346	121
Hattiban	27.655670	85.334410	121–122

**Table 5** Approximate locations of liquefaction evidence photographs provided in the Appendix

Table 6 Reference	Photo	Location	Latitude °N	Longitude °E	Evidence
3a	Figure 10	Bungmati	27.62886	85.29696	Cracking and sand boiling ejecta
3b	Figure 11	Bungmati	27.63028	85.29659	Cracking and sand boiling ejecta
6	Figure 12	Imadol	27.66614	85.33656	Tilted building
7a	Figure 4	Kausaltar	27.67473	85.36359	Ground fracture
7b	Figure 5a	Kausaltar	27.67512	85.36217	Tilted building
7c	Figure 5b	Kausaltar	27.67407	85.36265	Ground fracture

located near to boreholes locations in the SAFER/GEO-591 geo-database also reported in Fig. 2. In Fig. 2 the locations evidenced in the geotechnical extreme event reconnaissance (GEER) (Hashash et al. 2015 and Table 4) field studies are compared. Those that do not feature in Table 6, did not have an accompanying quality borehole record. In Table 5 the locations from this study are detailed, locations 7a, 7b and 7c represent new data collected in the aftermath of the Gorkha earthquake by the first author. All evidence data (i.e., photographic documentation and borehole details from SAFER/GEO-591) are provided in this paper (Tables 1, 4 and 5 and Figs. 10, 11, 12, 13, 14 and 15 in the Appendix). The  $P_L$  and the corresponding liquefaction potential category according to Iwasaki et al. (1984) and Sonmez (2003) are compared: both methodologies give similar computed values of liquefaction potential with Sonmez providing slightly higher  $P_L$  values (see Table 6) leading to a refined estimate. However, both estimates remain quite similar. Figure 4 shows a ground fissure at Kausaltar, Bhaktapur (Location 7a in Fig. 2), after the 2015 Gorkha earthquake. Figure 5a shows evidence of a building tilted due to liquefaction effects; this building was situated near the Araniko Highway, corresponding to Location 7b in Fig. 2. Figure 5b shows the liquefaction evidence record for Location 7c in Fig. 2.

**Table 6** Comparison of  $P_L$  values calculated using Iwasaki et al. (1984) and Sommez (2003)

Liq Ev ID	LOCA-ID	Approx. BH Easting	Approx. BH Northing	Earthquake Event	PGA <sup>1</sup>	Water table depth (m)	$P_L$ and corresponding Liquefaction potential category		Source of Evidence	Approx. Distance (m) from evidence point
							Iwasaki et al. (1984)	Sommez (2003)		
1	R_JRAP_2016_BH1 Manamaiju	334046.662	3071675.13	2015 Gorkha	0.32	0	57.26 (Very High)	57.26 (Very High)	Photo/J-Rapid (2016)	350 m
2	R_JRAP_2016_BH4 Ramkot	327938.8658	3067214.142	2015 Gorkha	0.32	3	0 (Very Low)	0 (No)	J-Rapid (2016)	40 m
3a	Bungmati-BH1 (Jha et al. 2020)	331960.224	3057228.83	2015 Gorkha	0.32	1	18.77 (Very High)	18.77 (Very High)	Photo (Fig. 10) <sup>2</sup> /Jha et al. (2020)	20 m
3b	Bungmati-BH2 (Jha et al. 2020)	332048.595	3057342.61	2015 Gorkha	0.32	2	4.61 (Low)	4.77 (Moderate)	Photo (Fig. 11) <sup>2</sup> /Jha et al. (2020)	180 m
4	R_JRAP_2016_BH2 NEC	343792.718	3066158.07	2015 Gorkha	0.28	3	1.46 (Low)	1.56 (Low)	Photo/J-Rapid (2016)	500 m
5	RES_Kate_1996_R1	333901.06	3065759.89	1934 Bihar-Nepal	0.34	2	11.45 (High)	11.61 (High)	Photo/Rana (1935) and Borehole data from Katel et al. (1996)	Vicinity <sup>3</sup>
6	R_JRAP_2016_BH3	336391.728	3061845.01	2015 Gorkha	0.32	0	18.42 (Very High)	18.69 (Very High)	Photo (Fig. 12)/J-Rapid (2016)	550 m
7a	IND_Kaus_2017_BH1	338684.695	3,062,300.184	2015 Gorkha	0.28	4	10.04 (High)	10.17 (Very High)	Photo (Fig. 4) <sup>2</sup>	37 m
7b	IND_Kaus_2017_BH2	338540.523	3062308.386	2015 Gorkha	0.28	4	6.73 (High)	6.73 (High)	Photo (Fig. 5a) <sup>2</sup>	38 m
7c	IND_Kaus_2017_BH3	338462.801	3062136.235	2015 Gorkha	0.28	4	8.16 (High)	8.16 (High)	Photo (Fig. 5b) <sup>2</sup>	55 m/40m <sup>4</sup>
<i>No liquefaction</i>										
8	RES_Pokh_2006_BH6	332560.105	3059972.86	2015 Gorkha	0.32	4	0 (Very Low)	0 (Non Liquefiable)	No liquefaction observed (Fig. 13)	

**Table 6** (continued)

Liq Ev ID	LOCA-ID	Approx. BH Easting	Approx. BH Northing	Earthquake Event	PGA <sup>1</sup>	Water table depth (m)	$P_L$ and corresponding liquefaction potential category	Source of Evidence	Approx. Distance (m) from evidence point
9	IND_Jaga_2010_BH1	344989.017	3061115.97	2015 Gorkha	0.28	4	0 (Very Low)	No liquefaction observed (Fig. 14)	
10	IND_Solt_2008a_BH1	332025.877	3065281.48	2015 Gorkha	0.28	4	0 (Very Low)	No Liquefaction observed (Fig. 15)	

<sup>1</sup>For the Gorkha earthquake PGA was estimated from the USGS Shakemap of the April 25, 2015 event, for 1934 Bihar-Nepal PGA was estimated from a macro-seismic map (Sapkota et al 2016) and regression curve (Wald et al. 1999)

<sup>2</sup>The photo evidence was collected by the first author in the aftermath of the Gorkha earthquake, see the Appendix; the same liquefaction location was also documented in another study (Jha et al. 2020)

<sup>3</sup>This is an historical record with location name (Tundikhel) on photograph, there is only one Tundikhel in Kathmandu. The photo reflects the location of the liquefaction evidence, but the exact distance cannot be determined

<sup>4</sup>Two photos available for evidence at the same site

**Fig. 4** Liquefaction and cracks in the ground at Kausaltar, Bhaktapur, Nepal, after the 2015 Gorkha earthquake, (Location 7a on Fig. 2). Photograph taken on 2015-05-31 [RM Pokhrel]



Photographic evidence collected by the first author in the aftermath of Gorkha earthquake and located in the vicinity of three boreholes from the SAFER/GEO-591 database (Gilder et al. 2019b) showed no evidence of liquefaction. These locations are indicated as 8, 9 and 10 in Table 6 are employed as “evidence of no liquefaction” to compare the performances of the two approaches of Iwasaki et al. (1984) and Sonmez (2003). For all three IDs 8, 9 and 10, the resulting  $P_L$  value is 0 predicting *very low* and *non-liquefiable* potential categories for Iwasaki et al. (1984) and Sonmez (2003), respectively (see Table 6).

### 3.3 Zoning

Sonmez’s (2003) methodology was found to be better suited for classification of computed  $P_L$  values based on the evidence presented in this paper for the Kathmandu Valley. Application of the methodology can provide  $P_L$  estimates at 75 discrete locations using SAFER/GEO-591 (Gilder et al. 2019b) (see Table 1 for a list of the boreholes used from SAFER/GEO-591). The final number of boreholes employed is due to the selection of higher quality investigations i.e., the deepest boreholes are used with availability of other geotechnical information) when multiple investigations are available at the same site. To draw liquefaction potential maps for the region kriging interpolation can be used. Kriging interpolation allows for the degree of variation among known data points and corresponding distance to estimate values in unknown areas (e.g., Baise et al. 2006; Thompson et al. 2010; Chung and Rogers 2011; Pokhrel et al. 2012, 2013; Thompson et al. 2014). In this paper, the adopted algorithm is the ordinary kriging approach implemented in ArcGIS (ESRI 2012). Given kriging is an interpolation method and that soils are highly variable the results from the maps shown in this paper should not be used for site-specific design work but rather as a useful guide for planning future infrastructure developments.

## 4 Liquefaction potential map for Kathmandu Valley

### 4.1 Seismic hazard

PGA values for the Kathmandu Valley are those based on the PSHA results provided by Stevens et al. (2018). As discussed in several studies (e.g., Stevens et al. 2018; Pokhrel

et al. 2019b; De Risi et al. 2020), the hazard in the region is dominated by the MHT; however, the study by Stevens et al. (2018) considered several additional sources contributing to the hazard. Furthermore, the assumption related to the GMPEs in the PSHA can significantly affect hazard results. There remains significant uncertainty related to the choice of GMPEs for PSHA studies in the Himalayan region and the lack of regional GMPEs supported by a significant number of data (e.g., Bajaj and Anbazhagan 2019). Stevens et al. (2018) employed an equally weighted logic tree in their PSHA, i.e., using an average of four GMPEs. Additionally, each GMPE was considered separately (data available in Stevens 2020).

The PGA maps for a probability of exceedance of 2% and 10% in 50 years are considered as they refer to the near-collapse and life safety reference in many international seismic codes (e.g., CEN 2004). The estimates of PGA employed for the Kathmandu Valley in this study are: (i) the final values provided in Stevens et al. based on the average of the four GMPEs considered defined as AVERAGE in the following and (ii) the PGA estimate resulting from the use of the GMPE from Atkinson and Boore (2003) indicated in the following as AB03. The first assumption was the inclusion of GMPEs suitable for crustal and subduction zones, and none of them being region-specific for the Himalaya given the lack of data and the further necessity to develop reliable GMPEs for the area (see also Bajaj and Anbazhagan 2019). The second assumption refers to the subduction GMPE proposed by Atkinson and Boore (2003), which is not region-specific but can be used as a lower bound for PGA for the Kathmandu Valley. Figures 6 and 7 show the PGA maps for the 2% and 10% in 50 years probability of exceedance considering both the AVERAGE (Fig. 6) and AB03 (Fig. 7) GMPE assumptions. Both PGA maps were calculated accounting for the local soil amplification in the basin. This was achieved using the  $V_{S30}$  used as the parameter for soil characterization using the GMPEs. The source for  $V_{S30}$  used in the GMPEs for the PSHA study (Stevens et al. 2018) was the USGS slope-based study by Wald and Allen (2007) and Allen and Wald (2009). This approach tends to overestimate the  $V_{S30}$  values (i.e. soil-stiffness) with respect to direct measurements, as shown in Gilder et al. (2018). For the geomorphological condition and complex geology of the Kathmandu Valley, the slope model does not represent an accurate approximation of  $V_{S30}$  (De Risi et al. 2021) but it is considered suitable at this stage for the scope of zoning liquefaction potential.



**Fig. 5** **a** Partial collapse due to tilting and seismic pounding in the Kausaltar area (Location 7b in Fig. 2) after the Gorkha earthquake; **b** liquefaction and cracks in the ground near the Araniko Highway at Kausaltar, Bhaktapur, as a result of the Gorkha Earthquake 2015, (Location 7c on Fig. 2). Photograph taken on 2015-05-31 [RM Pokhrel]

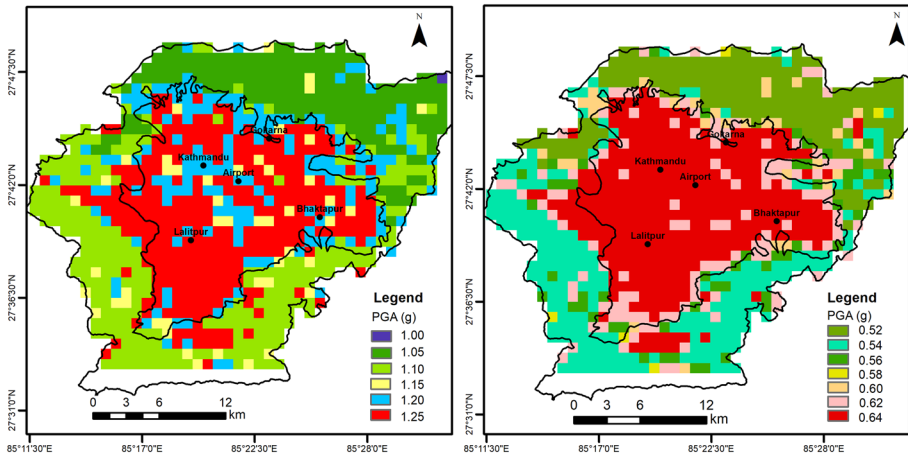


**Fig. 6** PGA map (horizontal component) of the Kathmandu Valley for **a** (left) 2% in 50 years probability of exceedance and **b** (right) 10% in 50 years probability of exceedance assuming the AVERAGE GMPE model choice by Stevens (2020) (data from Stevens 2020)

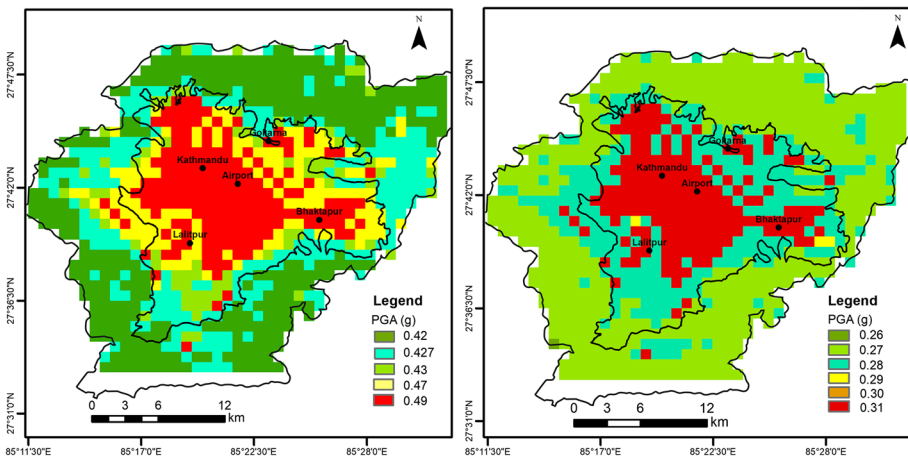


**Fig. 7** PGA map (horizontal component) of the Kathmandu Valley for **a** (left) 2% in 50 years probability of exceedance and **b** (right) 10% in 50 years probability of exceedance assuming the AB03 GMPE as provided by Stevens (2020) (data from Stevens 2020)

### 4.2 Results and discussion

The results are presented for a range of PGA values, obtained from an average representing several GMPEs, (GMPE AVERAGE of Stevens 2020) and a single GMPE (AB03 of Stevens 2020) as shown in Fig. 6 and Fig. 7. These figures indicate the uncertainty in the prediction. The geographical resolution of the data is at the order of approximately 1000 m.

At each borehole location in the SAFER/GEO-591 database used for the liquefaction potential analysis, two different seasonal values of water table depth were used (1.6 m and 5.1 m) as discussed in Sect. 2. Figure 8a and b show the liquefaction potential map of the



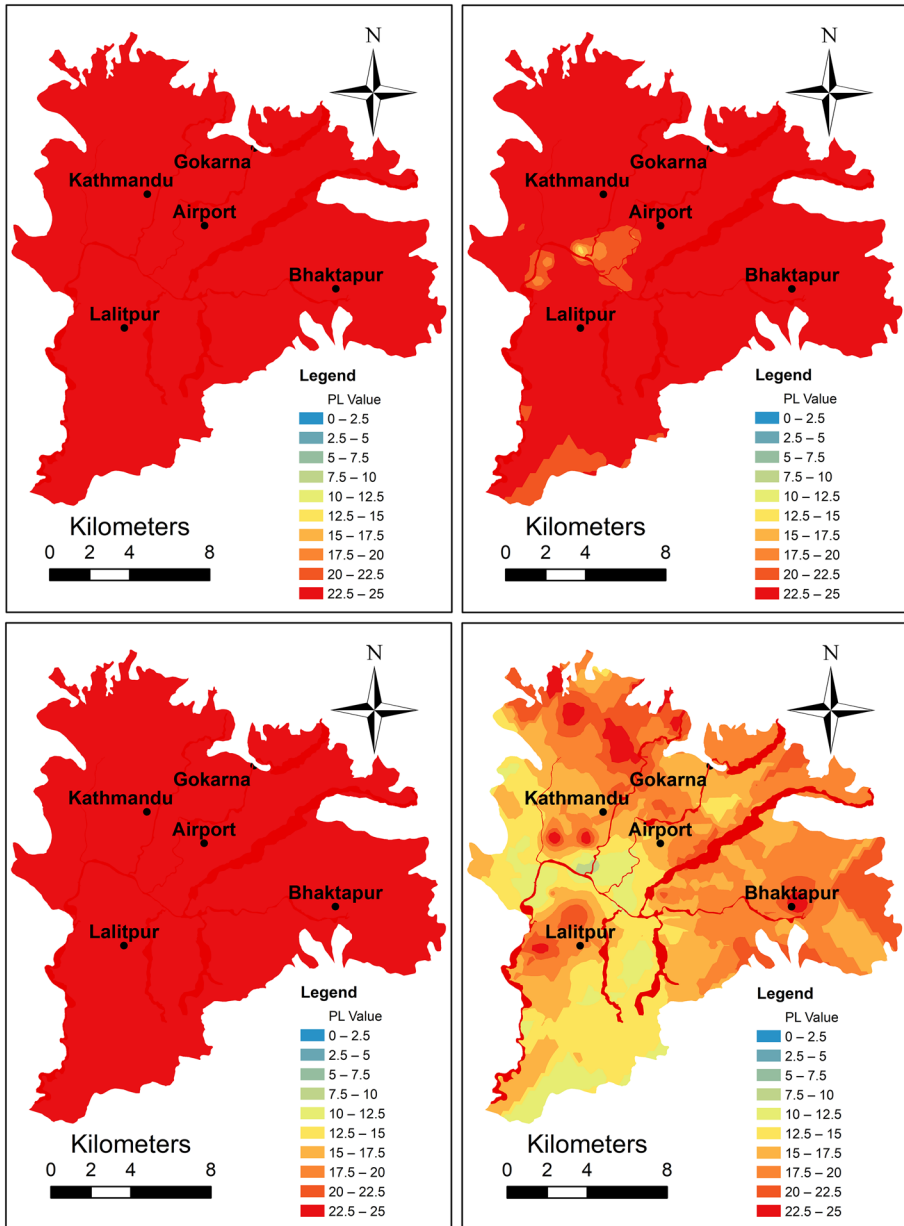


**Fig. 8** Liquefaction potential map of the Kathmandu Valley based on PGA assuming an AVERAGE GMPE for 2% in 50 years probability of exceedance under a **a** (top-left) wet scenario and **b** (top-right) dry scenario and for 10% in 50 years probability of exceedance in a **c** (bottom-left) wet scenario and **d** (bottom-right) dry scenario, respectively

Kathmandu Valley based on PGA considering the AVERAGE GMPE assumption for 2% in 50 years probability of exceedance under a *wet* scenario and *dry* scenario, respectively.



Similarly, Fig. 8c and d present 10% in 50 years probability of exceedance in a *wet* scenario and *dry* scenario, respectively. Among these, the PGA having 2% probability of exceedance in 50 years is around 1.2 g, and it is almost uniform across the valley. This represents the worst-case scenario of a wet season earthquake where both the sandy deposits and silty or fine-grained materials (characterizing the southern valley) are saturated and so have the potential to liquefy. On the other hand, the PGA for a probability of exceedance of 10% in 50 years is around 0.65 g, and it is more spatially variable (i.e., borehole to borehole). Severe liquefaction is anticipated all around the Kathmandu valley for these PGA values and with an assumed depth of groundwater table of 5.1 m during the dry season. In this scenario, most of the Kathmandu Valley has a high computed potential for liquefaction. Similarly, Fig. 9a and b present liquefaction potential maps of the Kathmandu Valley based on PGA considering only the *AB03* GMPE for 2% in 50 years probability of exceedance under a *wet* scenario and *dry* scenario, respectively. Figure 9c and d show the liquefaction potential for 10% probability of exceedance in 50 years in a *wet* scenario and *dry* scenario, respectively. The estimated PGA for the 2% probability of exceedance in 50 years is about 0.48 g and for 10% it is about 0.3 g, closer to the current design PGA in the Nepalese building code (NBC 2020).

An important geotechnical aspect is the superficial geology, the liquefiable layers are due to the presence of the river (supported by the GEER evidence, Hashash et al. 2015). However, when considering the distribution of the liquefaction potential in Fig. 8d in the central Valley, most areas correspond with the Somnez designation ‘moderate’ when located adjacent to the river edge. Two boreholes located between Kathmandu and Lalitpur either side of the river help evidence this result, and this probably is due to the dominant silt and clay-like materials often present at depth at these locations. The spatial position of these points (and the kriging results) gives lower values of potential liquefaction. As this indicates the ‘dry scenario’, the saturation in such deposits will be lower. Considering the laminated nature of the deposits and the fact that many locations are without borehole data, the results presented in this work are preliminary.

The flood plain areas have been identified and considered as having a high liquefaction potential used as a working assumption in all maps. The Gokarna and Tokha Formations at the northern part of the valley contain sand-dominant soil (Fujii and Sakai 2002 and Fig. 2). The Kalimati Formation dominantly comprises clayey silt has a lower liquefaction potential (Fujii and Sakai 2002). The liquefaction potential maps for all cases show that the northern part (Gokarna Formation) has a higher liquefaction potential than the southern (Kalimati Formation) region which complies with expectations considering the dominant constituents of these two materials. This result is expected given the geological nature of the deposits (the Kalimati is mainly clay while the Gorkarna is mainly sand). However, the original liquefaction expectation map shown in Shrestha et al. (1998) (see Fig. 1a) does not follow the geological expectation in the same way as the analysis presented here, or that of Piya (2004) and Piya et al. (2004) when based upon on a database containing more recent ground investigations (Gilder et al. 2019b, 2020).

No severe liquefaction was observed in the Kathmandu Valley during the Gorkha earthquake as discussed in previous studies (e.g., Chiaro et al. 2015; Moss et al. 2017). Based on the present study, this can be attributed to the season of the year in which the Gorkha earthquake occurred. April is peak dry season in the Kathmandu Valley (Fig. 8d). Most of the area in this season has a low potential for liquefaction, therefore, this result matches with the relatively limited evidence of liquefaction damage during that earthquake. If a similar, or larger, earthquake occurred in the future during peak wet season, the soil is expected to liquefy more significantly as shown in the Figs. 8a and c and 9a and c.

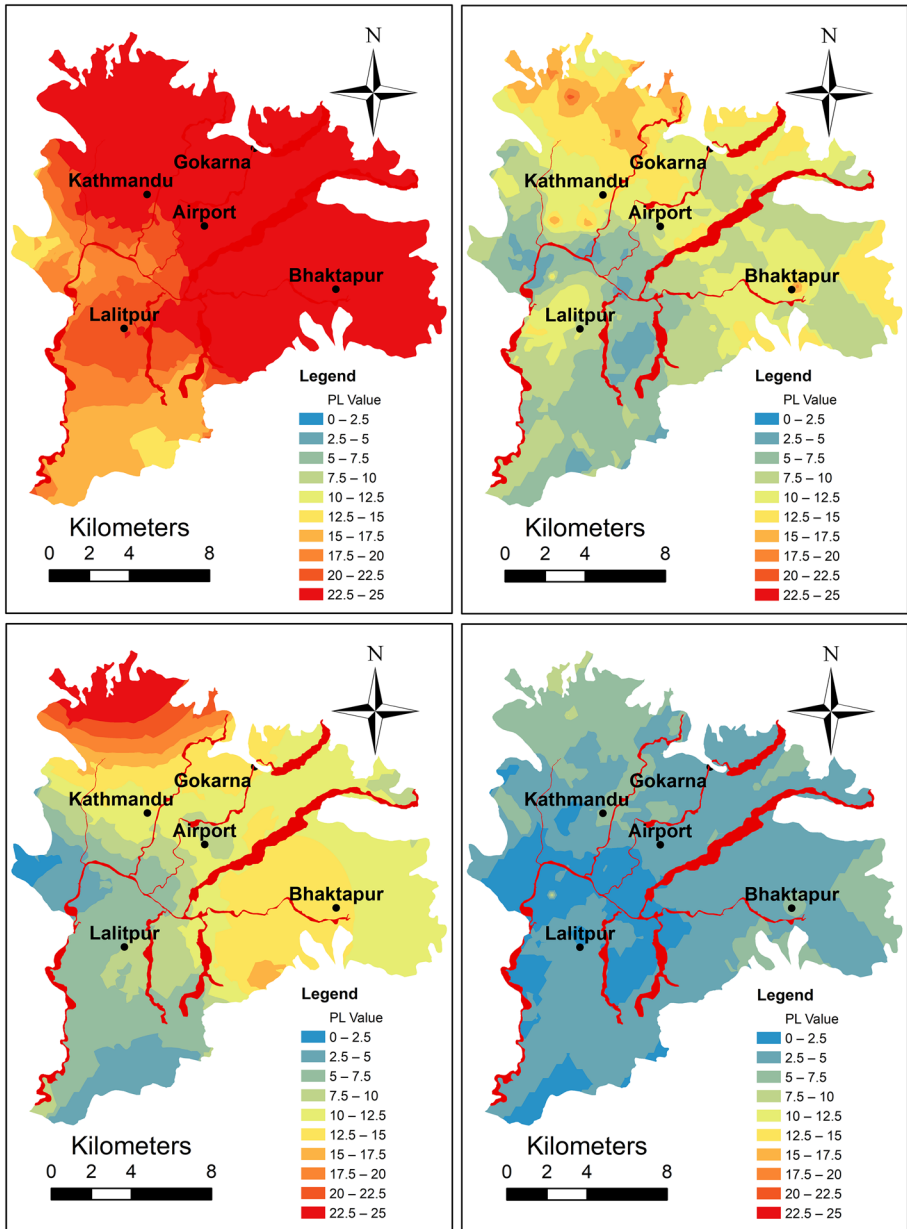


**Fig. 9** Liquefaction potential map of the Kathmandu Valley based on PGA assuming the AB03 GMPE for 2% in 50 years probability of exceedance under a **a** (top-left) wet scenario and **b** (top-right) dry scenario and for 10% in 50 years probability of exceedance in a **c** (bottom-left) wet scenario and **d** (bottom-right) dry scenario, respectively

## 5 Summary and conclusions

Liquefaction potential zoning maps are useful tools for seismic hazard assessment. In this study, information compiled from geo-database SAFER/GEO-591 was employed to develop new maps of liquefaction potential using SPT data. Notwithstanding the additional information provided by the database, the area of the valley is still not well characterized from a geotechnical perspective and therefore interpolation by ordinary kriging was used to obtain continuous hazard maps of liquefaction potential, developed for different scenarios of hazard-consistent PGA. The following conclusions are drawn:

- (a) The effect of changing depth of the water table to simulate seasonal variation was studied which is shown to have a significant effect on the distribution of computed liquefaction potential. This confirms the observations made by Moss et al. (2017) and highlights the need for season-dependent liquefaction susceptibility studies. This is an important issue as it further affects the predictions of structural and infrastructure damage in Kathmandu valley, which are key elements of regional loss assessment.
- (b) As expected, the scenario of shallow water table typical of the monsoon season is characterized by higher calculated liquefaction potential with respect to the dry season scenario.
- (c) The Gokarna Formation appears to have the highest computed potential for liquefaction with respect to other geological formations studied, which has resulted in maps that indicate higher liquefaction potential in the north of the valley compared to the south (where the composition is more cohesive).

To further refine the above observations, site response analyses at the city level can be performed to calculate the cyclic stress ratio in a more refined manner (De Risi et al. 2019). Currently the liquefaction potential maps are reliant on the available borehole distribution, and it should be noted that some areas are currently not well characterized (e.g., Bhaktapur). It is also expected that the assessment of liquefaction potential of the southernmost valley may increase with data from further investigations if the area is underlain by both weathered fan and deltaic deposits (Sakai et al. 2016). More recent work on liquefaction potential has investigated the role that silts might have on liquefaction potential (Shuttle and Cunning 2007). This may inform further work which may benefit future liquefaction potential studies for the Kathmandu Valley, given the central, most populated parts of the valley are underlain by potentially loose, saturated silts. Further work is also needed to compare the exact locations of observed liquefaction against the results predicted in this work. However, this study has shown the value of the SAFER/GEO-591 (Gilder et al. 2019b) database for regional estimates of liquefaction potential which may be useful for planning and loss assessment purposes.

## Appendix

See Figs. 10, 11, 12, 13, 14 and 15.

**Fig. 10** Liquefaction and sand boiling at Bungmati (Liq. ID 3a in Table 6) [Photo: RM Pokhrel]



**Fig. 11** Liquefaction and sand boiling at Bungmati (Liq. ID 3b in Table 6) [Photo: RM Pokhrel]





**Fig. 12** Tilted building due to liquefaction at Imadol (Liq. ID 6 in Table 6) [Photo: RM Pokhrel]



**Fig. 13** Structure damage observed at Bungmati village near Bhainsepati—no evidence of liquefaction (Liq. ID 8 in Table 6) [Photo: RM Pokhrel]



**Fig. 14** Structure damage observed at Jagati—no evidence of liquefaction (Liq. ID 9 in Table 6) [Photo: RM Pokhrel]



**Fig. 15** Structural damage observed at Kalanki near Solti—no evidence of liquefaction (Liq. ID 10 in Table 6) [Photo: RM Pokhrel]

**Funding** The authors acknowledge the support from the Engineering and Physical Science Research Council (EPSRC) project ‘Seismic Safety and Resilience of Schools in Nepal’ SAFER (EP/P028926/1). The second author acknowledges the support of EPSRC (EP/R51245X/1).

**Data availability and material** The PGA data used in this study can be downloaded from Stevens (2020) ([https://vickystevens.shinyapps.io/Nepal\\_seismichazard/](https://vickystevens.shinyapps.io/Nepal_seismichazard/)) and the SAFER/GEO-591 data can be downloaded from Gilder et al. (2019b) (<https://doi.org/10.5523/bris.3gcvx51lnpuv269xsa1yrb0rw>).

**Conflict of interest** The authors declare that they have no conflict of interest.

**Open Access** This article is licensed under a Creative Commons Attribution 4.0 International License, which permits use, sharing, adaptation, distribution and reproduction in any medium or format, as long as you give appropriate credit to the original author(s) and the source, provide a link to the Creative Commons

licence, and indicate if changes were made. The images or other third party material in this article are included in the article's Creative Commons licence, unless indicated otherwise in a credit line to the material. If material is not included in the article's Creative Commons licence and your intended use is not permitted by statutory regulation or exceeds the permitted use, you will need to obtain permission directly from the copyright holder. To view a copy of this licence, visit <http://creativecommons.org/licenses/by/4.0/>.

## References

- Allen TI, Wald DJ (2009) On the use of high-resolution topographic data as a proxy for seismic site conditions (VS30). *Bull Seismol Soc Am* 99(2A):935–943. <https://doi.org/10.1785/0120080255>
- Atkinson GM, Boore DM (2003) Empirical ground-motion relations for subduction zone earthquakes and their applications to Cascadia and other regions. *Bull Seismol Soc Am* 93(4):1703–1729. <https://doi.org/10.1785/0120020156>
- Baise LG, Lenz JA (2006) Guidelines for regional liquefaction hazard mapping. *Final technical report for U.S. Geological survey award No. 05HQGR0103*, United States Geological Survey, Reston, VA, USA.
- Bajaj K, Anbazhagan P (2019) Regional stochastic GMPE with available recorded data for active region—Application to the Himalayan region. *Soil Dyn Earthq Eng* 126:105825. <https://doi.org/10.1016/j.soildyn.2019.105825>
- Baker JW, Faber MH (2008) Liquefaction risk assessment using geostatistics to account for soil spatial variability. *J Geotech Geoenviron Eng (ASCE)* 134(1):14–23. [https://doi.org/10.1061/\(ASCE\)1090-0241\(2008\)134:1\(14\)](https://doi.org/10.1061/(ASCE)1090-0241(2008)134:1(14))
- Bilham R (1995) Location and magnitude of the 1833 Nepal earthquake and its relation to the rupture zones of contiguous great Himalayan earthquakes. *Curr Sci* 69(2):101–128
- Bilham R (2019) Himalayan earthquakes: a review of historical seismicity and early 21st century slip potential. *Geol Soc, London, Spl Publ* 483:423–482. <https://doi.org/10.1144/SP483.16>
- Central Bureau of Statistics (CBS) (2012). National Population and Housing Census 2011, National Report, Government of Nepal, November 2012.
- Chaulagain H, Rodrigues H, Silva V, Spacone E, Varum H (2015) Seismic risk assessment and hazard mapping in Nepal. *Nat Hazards* 78(1):583–602. <https://doi.org/10.1007/s11069-015-1734-6>
- Chen WP, Molnar P (1977) Seismic moments of major earthquakes and the average rate of slip in central Asia. *J Geophys Res* 82(20):2945–2969. <https://doi.org/10.1029/JB082i020p02945>
- Chiaro G, Kiyota T, Pokhrel RM, Goda K, Katagiri T, Sharma K (2015) Reconnaissance report on geotechnical and structural damage caused by the 2015 Gorkha Earthquake, Nepal. *Soils Found* 55(5):1030–1043. <https://doi.org/10.1016/j.soildyn.2015.09.006>
- Chung JW, Rogers JD (2011) Simplified method for spatial evaluation of liquefaction potential in the St. Louis area. *J Geotech Geoenviron Eng (ASCE)* 137(5):505–515. [https://doi.org/10.1061/\(ASCE\)GT.1943-5606.0000450](https://doi.org/10.1061/(ASCE)GT.1943-5606.0000450)
- De Risi R, De Luca F, Gilder CEL, Pokhrel RM, Vardanega PJ (2021) The SAFER geodatabase for the Kathmandu valley: Bayesian kriging for data-scarce regions. *Earthq Spectra* 37(2):1108–1126. <https://doi.org/10.1177/8755293020970977>
- De Risi R, Wang S, Werner MJ, De Luca F, Vardanega PJ, Pokhrel RM, Maskey PN, Sextos A (2020) Simulation-based PSHA for the Kathmandu Valley: Sensitivity to hypocentre randomisation. In: *Proceedings of the 17th world conference on earthquake engineering (17WCEE)*, Paper No. 1c-0040. 9pp.
- De Risi R, Penna A, Simonelli AL (2019) Seismic risk at urban scale: the role of site response analysis. *Soil Dyn Earthq Eng* 123:320–336. <https://doi.org/10.1016/j.soildyn.2019.04.011>
- Elliott JR, Jolivet R, González PJ, Avouac JP, Hollingsworth J, Searle MP, Stevens VL (2016) Himalayan megathrust geometry and relation to topography revealed by the Gorkha earthquake. *Nat Geosci* 9(2):174–180. <https://doi.org/10.1038/NGEO2623>
- Environmental Systems Research Institute (ESRI) (2012). ArcGIS 10.1. Environmental Systems Research Institute, Redlands, CA, USA.
- European Committee for Standardization (CEN) (2004) Eurocode 8: Design of Structures for Earthquake Resistance—Part 1: General rules, seismic actions and rules for buildings. CEN, Brussels
- Fan Y, Li H, Miguez-Macho G (2013) Global patterns of groundwater table depth. *Science* 339(6122):940–943. <https://doi.org/10.1126/science.1229881>
- Fujii R, Sakai H (2002) Paleoclimatic changes during the last 2.5 myr recorded in the Kathmandu Basin, Central Nepal Himalayas. *J Asian Earth Sci* 20(3):255–266. [https://doi.org/10.1016/S1367-9120\(01\)00048-7](https://doi.org/10.1016/S1367-9120(01)00048-7)

- Gautam D, de Magistris FS, Fabbrocino G (2017) Soil liquefaction in Kathmandu valley due to 25 April 2015 Gorkha, Nepal earthquake. *Soil Dyn Earthq Eng* 97:37–47. <https://doi.org/10.1016/j.soildyn.2017.03.001>
- Geyin M, Baird AJ, Maurer BW (2020) Field assessment of liquefaction prediction models based on geotechnical versus geospatial data, with lessons for each. *Earthq Spectra* 36(3):1386–1411. <https://doi.org/10.1177/8755293019899951>
- Gilder CEL, De Risi R, De Luca F, Vardanega PJ, Holcombe EA, Ayoubi P, Asimaki D, Pokhrel RM, Sextos A (2018) Optimising resolution and improvement strategies for emerging geodatabases in developing countries. In: *Proceedings of the 16<sup>th</sup> European conference on earthquake engineering*, european association for earthquake engineering (EAEE), Paper No. 10743.
- Gilder CEL, Pokhrel RM, Vardanega PJ (2019a) A ground investigation to inform earthquake hazard assessment in the Kathmandu Valley, Nepal. In: *17<sup>th</sup> European conference on soil mechanics and geotechnical engineering*, (XVII ECSMGE-2019), Reykjavik, Iceland, < [https://www.ecsmge-2019.com/uploads/2/1/7/9/2/1790806/0110-ecsmge-2019\\_gilder.pdf](https://www.ecsmge-2019.com/uploads/2/1/7/9/2/1790806/0110-ecsmge-2019_gilder.pdf) > (14/06/2021)
- Gilder CEL, Pokhrel RM, Vardanega PJ (2019b) *The SAFER Borehole database (SAFER/GEO-591): User manual, December 2019, v1.1*. University of Bristol, Bristol, UK. <https://doi.org/10.5523/bris.3gjcvx51lnpuv269xsa1yrb0rw>
- Gilder CEL, Pokhrel RM, Vardanega PJ, De Luca F, De Risi R, Werner MJ, Asimaki D, Maskey PN, Sextos A (2020) The SAFER geodatabase for the Kathmandu Valley: geotechnical and geological variability. *Earthq Spectra* 36(3):1549–1569. <https://doi.org/10.1177/8755293019899952>
- Gilder CEL, Pokhrel RM, De Luca F, Vardanega PJ (2021) Insights from CPTu and seismic cone penetration testing in the Kathmandu Valley, Nepal. *Front Built Environ* 7:646009. <https://doi.org/10.3389/fbuil.2021.646009>
- Goda K, Kiyota T, Pokhrel RM, Chiaro G, Katagiri T, Sharma K, Wilkinson S (2015) The 2015 Gorkha Nepal earthquake: insights from earthquake damage survey. *Front Built Environ* 1:8. <https://doi.org/10.3389/fbuil.2015.00008>
- Grandin R, Vallée M, Satriano C, Lacassin R, Klinger Y, Simoes M, Bollinger L (2015) Rupture process of the Mw= 7.9 2015 Gorkha earthquake (Nepal): insights into Himalayan megathrust segmentation. *Geophys Res Lett* 42(20):8373–8382. <https://doi.org/10.1002/2015GL066044>
- Habibullah BM, Pokhrel RM, Kuwano J, Tachibana S (2012) GIS-based soil liquefaction hazard zonation due to earthquake using geotechnical data. *Int J GEOMATE* 2(1):154–160
- Hashash YMA, Tiwari B, Moss RES, Asimaki D, Clahan KB, Kieffer DS, Dreger DS, Macdonald A, Madugo CM, Mason HB, Pehlivan M, Rayamajhi D, Acharya I, Adhikari B (2015) Geotechnical field reconnaissance: Gorkha (Nepal) Earthquake of April 25 2015 and Related Shaking Sequence. Geotechnical Extreme Event Reconnaissance GEER Association, *Report No. GEER-040*. Version 1.1. <https://doi.org/10.181118/G61591>
- Iwasaki T, Tatsuoka F, Tokida K, Yasuda S (1978) A practical method for assessing soil liquefaction potential based on case studies at various sites in Japan. In: *Proceedings of the 2nd International conference on microzonation*, San Francisco, CA, USA, vol. 2, pp. 885–896.
- Iwasaki T, Tokida K, Tatsuoka F, Watanabe S, Yasuda S, Sato H (1982) Microzonation for soil liquefaction potential using simplified methods. In: *Proceedings of 3rd International earthquake microzonation conference*, Seattle, pp. 1319–1330.
- Iwasaki T, Arakawa T, Tokida K (1984) Simplified procedures for assessing soil liquefaction during earthquakes. *Int J Soil Dyn Earthq Eng* 3(1):49–58. [https://doi.org/10.1016/0261-7277\(84\)90027-5](https://doi.org/10.1016/0261-7277(84)90027-5)
- Jha SK, Karki B, Bhattarai A (2020) Deterministic and probabilistic evaluation of liquefaction potential: a case study from 2015 Gorkha (Nepal) earthquake. *Geotech Geol Eng* 38(4):4369–4384. <https://doi.org/10.1007/s10706-020-01277-7>
- J-RAPID (2016). Japan-Nepal Urgent Collaborative Projects regarding the April 2015 Nepal earthquake within the J-Rapid Program: Investigation of foundation liquefaction susceptibility in the Kathmandu Valley, Final Report.
- Katel TP, Upreti BN, Pokharel GS (1996) Engineering properties of fine grained soils of Kathmandu Valley Nepal. *J Nepal Geol Soc* 14:121–138. <https://doi.org/10.3126/jngs.v14i0.32401>
- Khatakho R, Gautam D, Aryal KR, Pandey VP, Rupakhety R, Lamichhane S, Liu Y-C, Abdouli K, Talchabhadel R, Thapa BR, Adhikari R (2021) Multi-hazard risk assessment of Kathmandu Valley, Nepal. *Sustainability* 13(10):5369. <https://doi.org/10.3390/su13105369>
- Koester JP, Tsuchida T (1988) Earthquake-induced liquefaction of fine-grained soils—considerations from Japanese research. *Miscellaneous Paper GL-88-34*. US Army Corps of Engineers, Washington, DC, USA.
- Kottek M, Grisser J, Beck C, Rudolf B, Rubel F (2006) World map of the Koppen-Geiger climate classification updated. *Meteorologische Zeitschrift* 15(3):259–263. <https://doi.org/10.1127/0941-2948/2006/0130>



- Liu CN, Chen CH (2006) Mapping liquefaction potential considering spatial correlations of CPT measurements. *J Geotech Geoenviron Eng (ASCE)* 132(9):1178–1187. [https://doi.org/10.1061/\(ASCE\)1090-0241\(2006\)132:9\(1178\)](https://doi.org/10.1061/(ASCE)1090-0241(2006)132:9(1178))
- Liu CN, Chen CH (2010) Spatial correlation structures of CPT data in a liquefaction site. *Eng Geol* 111:43–50. <https://doi.org/10.1016/j.enggeo.2009.12.002>
- Liu F (2008) Data discovery on liquefaction-induced lateral ground deformations. *Ph.D. thesis*, University of Southern California, CA, USA.
- Maruyama Y, Yamazaki F, Mizuno K, Tsuchiya Y, Yogai H (2010) Fragility curves for expressway embankments based on damage datasets after recent earthquakes in Japan. *Soil Dyn Earthq Eng* 30(11):1158–1167. <https://doi.org/10.1016/j.soildyn.2010.04.024>
- Moss RES, Thompson EM, Kieffer DS, Tiwari B, Hashash YMA, Acharya I, Adhikari BR, Asimaki D, Clahan KB, Collins BD, Dahal S, Jibson RW, Khadka D, Macdonald A, Madugo CLM, Mason HB, Pehlivan M, Rayamajhi D, Upreti S (2015) Geotechnical effects of the 2015 magnitude 7.8 Gorkha, Nepal, earthquake and aftershocks. *Seismol Res Lett* 86(6):1514–1523. <https://doi.org/10.1785/0220150158>
- Moss RES, Baise LG, Zhu J, Kadkha D (2017) Examining the discrepancy between forecast and observed liquefaction from the 2015 Gorkha, Nepal, earthquakes. *Earthq Spectra* 33(S1):S73–S83. <https://doi.org/10.1193/120316EQS220M>
- Nepal National Building Code (NBC) (1994). Nepal National Building Code NBC 105:1994, Seismic Design of Buildings in Nepal. *Government of Nepal Ministry of Physical Planning and works, Department of Urban Development and Building Construction*. Babarmahal, Kathmandu, Nepal.
- Nepal National Building Code (NBC) (2020). Nepal National Building Code NBC 105:2020, Seismic Design of Buildings in Nepal. *Government of Nepal Ministry of Urban Development, Department of Urban Development and Building Construction*. Babarmahal, Kathmandu, Nepal.
- Pandey MR, Molnar P (1988) The distribution of intensity of the Bihar-Nepal earthquake 15 January 1934 and bounds of the extent of the rupture zone. *J Nepal Geol Soc* 5(1):22–44. <https://doi.org/10.3126/jngs.v5i1.32559>
- Pandey MR, Chitrakar GR, Kafle B, Sapkota SN, Rajaure S, Gautam UP (2002) *Seismic hazard map of Nepal*. Department of Mines and Geology, Kathmandu, Nepal.
- Pandey VP, Shrestha S, Kazama F (2012) Groundwater in the Kathmandu Valley: development dynamics, consequences and prospects for sustainable management. *Eur Water* 37:3–14
- Paudel MR, Sakai H (2009) Stratigraphy and depositional environment of late Pleistocene Sunakothi Formation in Kathmandu Basin, Central Nepal. *J Nepal Geol Soc* 39:33–44. <https://doi.org/10.3126/jngs.v39i0.31486>
- Piya BK (2004) Generation of a geological database for the liquefaction hazard assessment in Kathmandu Valley. *M.Sc. thesis*, International Institute for Geo-Information Science and Earth Observation, Enschede, The Netherlands.
- Piya B, Van Western C, Woldai T (2004) Geological database for liquefaction hazard analysis in the Kathmandu valley, Nepal. *J Nepal Geol Soc* 30:141–152. <https://doi.org/10.3126/jngs.v30i0.31704>
- Pokharel AK, Hallett J (2015) Distribution of rainfall intensity during the summer monsoon season over Kathmandu, Nepal. *Weather* 70(9):257–261. <https://doi.org/10.1002/wea.2544>
- Pokhrel R, Kuwano J, Tachibana S (2010) Liquefaction hazard zonation mapping of the Saitama City, Japan. *J Nepal Geol Soc* 40:69–76. <https://doi.org/10.3126/jngs.v40i0.23598>
- Pokhrel RM, Kuwano J, Tachibana S (2012) Geostatistical analysis for spatial evaluation of liquefaction potential in Saitama city. *Lowland Technol Int* 14(1):45–51
- Pokhrel RM, Kuwano J, Tachibana S (2013) A kriging method of interpolation used to map liquefaction potential over alluvial ground. *Eng Geol* 152(1):26–37. <https://doi.org/10.1016/j.enggeo.2012.10.003>
- Pokhrel RM, Gilder CEL, Vardanega PJ, De Luca F, Werner MJ, Maskey PN (2019a) Estimation of  $V_{S30}$  by HVSR method at a site in the Kathmandu Valley, Nepal. In: *2nd International conference on earthquake engineering and post disaster reconstruction planning (ICEE-PDRP)*, Bhaktapur, Nepal, pp. 52–60.
- Pokhrel RM, De Risi R, Werner M, De Luca F, Vardanega PJ, Maskey PN, Sextos A (2019b) Simulation-based PSHA for the Kathmandu Basin in Nepal. In: *13th International conference on applications of statistics and probability in civil engineering (ICASP13)*, Seoul, South Korea. < <http://hdl.handle.net/10371/153478> > (14/06/2021).
- Rajendran CP, John B, Rajendran K, Sanwal J (2016) Liquefaction record of the great 1934 earthquake predecessors from the north Bihar alluvial plains of India. *J Seismol* 20(3):733–745. <https://doi.org/10.1007/s10950-016-9554-z>
- Rana BS (1935) Nepal Ko Maha Bhukampa (The great earthquake of Nepal). Jorganesh Press, Kathmandu (in Nepali)

- Sajan KC, Bhochhibhoya S, Adhikari P, Adhikari P, Gautam D (2020) Probabilistic seismic liquefaction hazard assessment of Kathmandu valley, Nepal. *Geomat, Natural Hazards Risk* 11(1):259–271. <https://doi.org/10.1080/19475705.2020.1718220>
- Sakai H, Fuji R, Sugimoto M, Setoguchi R, Raj Paudel M (2016) Two times lowering of lake water at around 48 and 38ka, caused by possible earthquakes, recorded in the Paleo-Kathmandu lake, central Nepal Himalaya. *Earth, Planets Space*. <https://doi.org/10.1186/s40623-016-0413-5>
- Sakai T, Gajurel AP, Tabata H, Ooi N, Takagawa T, Kitagawa H, Upreti BN (2008) Revised lithostratigraphy of fluvio-lacustrine sediments comprising northern Kathmandu basin in central Nepal. *J Nepal Geol Soc* 37:25–44
- Sapkota SN, Bollinger L, Perrier F (2016) Fatality rates of the Mw~8.2, 1934, Bihar-Nepal earthquake and comparison with the April 2015 Gorkha earthquake. *Earth, Planets Space*. <https://doi.org/10.1186/s40623-016-0416-2>
- Seed HB, Idriss IM (1971) Simplified Procedure for Evaluating soil liquefaction potential. *J Soil Mech Found Div (ASCE)* 97(9):1249–1273
- Sharma K, Deng L (2019) Reconnaissance report on geotechnical engineering aspect of the 2015 Gorkha, Nepal, earthquake. *J Earthq Eng* 23(3):512–537. <https://doi.org/10.1080/13632469.2017.1342299>
- Shrestha P, Tamrakar NK (2013) Morphometry and geomorphic development of the Bagmati River Basin, Nepal Himalaya. *J Nepal Geol Soc* 46:41–56. <https://doi.org/10.3126/jngs.v46i0.31582>
- Shrestha M, Tamrakar NK (2018) Spatial variability of shallow groundwater level in the Northern Kathmandu Valley. *J Nepal Geol Soc* 55(1):45–54. <https://doi.org/10.3126/jngs.v55i1.22788>
- Shrestha OM, Koirala A, Karmacharya SL, Pradhananga UB, Pradhan R, Karmacharya R (1998) Engineering and environmental geological map of the Kathmandu Valley (1:50,000) Dept. Mines and Geology, His Majesty's Government of Nepal.
- Shuttle DA, Cuning J (2007) Liquefaction potential of silts from CPTu. *Can Geotech J* 44(1):1–19. <https://doi.org/10.1139/T06-086>
- Sonmez H (2003) Modification of the liquefaction potential index and liquefaction susceptibility mapping for a liquefaction-prone area (Inegol, Turkey). *Environ Geol* 44(7):862–871. <https://doi.org/10.1007/s00254-003-0831-0>
- Sonmez H, Gokceoglu C (2005) A liquefaction severity index suggested for engineering practice. *Environ Geol* 48(1):81–91. <https://doi.org/10.1007/s00254-005-1263-9>
- Stevens, V.L. (2020). PSHA of Nepal. Data-set available from < [https://vickystevens.shinyapps.io/Nepal\\_seismic\\_hazard/](https://vickystevens.shinyapps.io/Nepal_seismic_hazard/) > (accessed 30/06/2020).
- Stevens VL, Shrestha SN, Maharjan DK (2018) Probabilistic seismic hazard assessment of Nepal. *Bull Seismol Soc Am* 108(6):3488–3510. <https://doi.org/10.1785/0120180022>
- Szeliga W, Hough S, Martin S, Bilham R (2010) Intensity, magnitude, location, and attenuation in India for felt earthquakes since 1762. *Bull Seismol Soc Am* 100(2):570–584. <https://doi.org/10.1785/0120080329>
- Thompson EM, Baise LG, Kayen RE, Tanaka Y, Tanaka H (2010) A geostatistical approach to mapping site response spectral amplifications. *Eng Geol* 114(3–4):330–342. <https://doi.org/10.1016/j.enggeo.2010.05.010>
- Thompson EM, Wald DJ, Worden CB (2014) A VS30 map for California with geologic and topographic constraints. *Bull Seismol Soc Am* 104(5):2313–2321. <https://doi.org/10.1785/0120130312>
- Tsuchida, H. (1970). Prediction and Countermeasure against Liquefaction in Sand Deposits. Abstract of the Seminar of the Port and Harbour Research Institute, Ministry of Transport, Yokosuka, Japan, pp. 3.1–3.33 (In Japanese).
- UNDP/UNCHS (HABITAT). (1993). Seismic Hazard Mapping and Risk Assessment for Nepal. Prepared for Ministry of Housing and Physical Planning (MoHPP), His Majesty's Government of Nepal (HMG), the United Nations Development Programme (UNDP), United Nations Centre for Human Settlements (HABITAT) and Beca Worley International (New Zealand). In association with SILT Consultants, TAEC Consult, Golder Associates (Canada) and Urban Regional Research (USA). Report No. NEP/88/054/21.03.
- Valverde-Palacios I, Vidal F, Valverde-Espinosa I, Martín-Morales M (2014) Simplified empirical method for predicting earthquake-induced settlements and its application to a large area in Spain. *Eng Geol* 181:58–70. <https://doi.org/10.1016/j.enggeo.2014.08.009>
- Wald DJ, Allen TI (2007) Topographic slope as a proxy for seismic site conditions and amplification. *Bull Seismol Soc Am* 97(5):1379–1395. <https://doi.org/10.1785/0120060267>
- Wald DJ, Quitariano V, Heaton TH, Kanamori H (1999) Relationship between peak ground acceleration, peak ground velocity, and modified intensity in California. *Earthq Spectra* 15(3):557–564. <https://doi.org/10.1193/1.1586058>

- Yoshida M, Gautam P (1988) Magnetostratigraphy of Plio-Pleistocene lacustrine deposits in the Kathmandu Valley, Central Nepal. *Proceed Indian Nat Sci Acad* 54A(3):410–417
- Yoshida M, Igarashi Y (1984) Neogene to Quaternary lacustrine sediments in the Kathmandu Valley, Nepal. *J Nepal Geol Soc* 4:73–100

**Publisher's Note** Springer Nature remains neutral with regard to jurisdictional claims in published maps and institutional affiliations.

## Authors and Affiliations

Rama M. Pokhrel<sup>1</sup>  · Charlotte E. L. Gilder<sup>1</sup>  · Paul J. Vardanega<sup>1</sup>  ·  
Flavia De Luca<sup>1</sup>  · Raffaele De Risi<sup>1</sup>  · Maximilian J. Werner<sup>2</sup>  ·  
Anastasios Sextos<sup>1</sup> 

Rama M. Pokhrel  
pokhrelmohan@gmail.com

Charlotte E. L. Gilder  
cg9173@bristol.ac.uk

Flavia De Luca  
flavia.deluca@bristol.ac.uk

Raffaele De Risi  
raffaele.derisi@bristol.ac.uk

Maximilian J. Werner  
max.werner@bristol.ac.uk

Anastasios Sextos  
a.sextos@bristol.ac.uk

<sup>1</sup> Department of Civil Engineering, University of Bristol, Bristol, UK

<sup>2</sup> School of Earth Sciences, University of Bristol, Bristol, UK